Decentralized State Estimation and Bad Measurement Identification: An Efficient Lagrangian Relaxation Approach

Eduardo Caro, *Student Member, IEEE*, Antonio J. Conejo, *Fellow, IEEE*, and Roberto Mínguez

***Abstract*—This paper proposes a decentralized state-estimation approach that relies on an elaborated instance of the Lagrangian relaxation decomposition technique. The proposed algorithm does not require a central coordinator but just to moderate interchanges of information among neighboring regions, and exploits the structure of the problem to achieve a fast and accurate convergence. Additionally, a decentralized bad measurement identification procedure is developed, which is efficient and robust in terms of identifying bad measurements within regions and in border tie-lines. The accuracy and efficiency of the proposed procedures are assessed by a large number of simulations, which allows drawing statistically sound conclusions.**

***Index Terms*—State estimation, bad measurement identification, decentralization, Lagrangian relaxation.**

NOTATION

The main notation used throughout the paper is stated below for quick reference. Other symbols are defined as required.

A. Sets:

Ω_{A_i}	Set of regions adjacent to region A_i.
Θ_{bor}	Set of measurements corresponding to border lines.
Θ_{in}	Set of measurements corresponding to non-border lines.

B. Variables:

$\boldsymbol{V}$	Voltage magnitude vector.
$\boldsymbol{\theta}$	Voltage angle vector.
$\boldsymbol{x}$	State vector ($n \times 1$).
$\boldsymbol{x}_i$	State vector for region A_i.
$\boldsymbol{x}_i^{\text{I}}$	State vector of interior buses for region A_i.
$\boldsymbol{x}_i^{\text{B}}$	State vector of border buses for region A_i.

Note that $\boldsymbol{x}_i = [(\boldsymbol{x}_i^{\text{I}})^T(\boldsymbol{x}_i^{\text{B}})^T]^T$.

C. Parameters and Constants:

ε	Tolerance.
n	Number of state variables.
n_A	Number of regions.
m	Number of measurements.
$\boldsymbol{x}^{\text{true}}$	True state vector ($n \times 1$).
$\boldsymbol{z}$	Measurement vector ($m \times 1$).
$\boldsymbol{W}$	Weighting matrix ($m \times m$).

D. Functions:

$\boldsymbol{h}$	Functional vector ($m \times 1$) that relates measurements and state variables.
$\boldsymbol{f}$	Equality constraint vector.
$\boldsymbol{g}$	Inequality constraint vector.
$\boldsymbol{f}_i$	Equality constraint vector for region A_i.
$\boldsymbol{g}_i$	Nonlinear inequality constraint vector for region A_i.
$\boldsymbol{f}_{ij}$	Equality constraint vector corresponding to the inter-regional zone $A_i - A_j$.
$\boldsymbol{g}_{ij}$	Nonlinear inequality constraint vector corresponding to the inter-regional zone $A_i - A_j$.
J	Objective function.

E. Optimization Vectors and Matrices:

$\boldsymbol{x}^*$	Estimated state vector ($n \times 1$).
$\boldsymbol{r}$	Residual vector ($m \times 1$).
$\boldsymbol{r}^N$	Normalized residual vector ($m \times 1$).
$\boldsymbol{\Omega}$	Residual variance-covariance matrix ($m \times m$).
$\boldsymbol{H}$	Jacobian matrix ($m \times n$).
$\boldsymbol{\lambda}_i$	Lagrangian multiplier vector of constraints $\boldsymbol{f}_i$.
$\boldsymbol{\mu}_i$	Lagrangian multiplier vector of constraints $\boldsymbol{g}_i$.
$\boldsymbol{\lambda}_{ij}^{\text{B}}$	Lagrangian multiplier vector of constraints $\boldsymbol{f}_{ij}$.
$\boldsymbol{\mu}_{ij}^{\text{B}}$	Lagrangian multiplier vector of constraints $\boldsymbol{g}_{ij}$.

I. INTRODUCTION

A. Motivation and Aim

MARKET operation in each national (e.g., in Europe) or regional (e.g., in the US) system of an interconnected multi-regional system calls for an increasingly accurate knowledge of the state of each national/regional system. This requires increasingly efficient state-estimation tools to be used by the Transmission System Operator (TSO) of each interconnected region. An accurate estimation of the system state in each interconnected region is of high importance to ensure a secure and economically efficient operation of each regional electric energy system and of the interconnected system as a whole.

As interconnections among regions become stronger, the system state in a given region needs to be estimated considering in a precise manner the interactions of other regions, but

E. Caro, A. J. Conejo, and R. Mínguez are partly supported by Junta de Comunidades de Castilla–La Mancha through project POII11-0102-0275 and by the Ministry of Education and Science of Spain through CICYT Project DPI2009-09573. R. Mínguez is partly supported by the Spanish Ministry of Science and Innovation through the Ramon y Cajal program.

E. Caro and A. J. Conejo are with Univ. Castilla–La Mancha, Ciudad Real, Spain (e-mails: Eduardo.Caro@uclm.es, Antonio.Conejo@uclm.es).

R. Mínguez is with the Environmental Hydraulics Institute IH Cantabria, Univ. de Cantabria, Cantabria, Spain (e-mail: Roberto.Minguez@unican.es).

minimizing the exchanged information between them. Hence, decentralized state-estimation algorithms become important tools.

This paper proposes a state-estimation procedure that allows estimating the state of each regional system of a multi-regional system in a decentralized manner. The final estimate is identical to that that would be obtained by a central operator using the whole information available in all regional systems.

The proposed decomposition is not oriented to improve computational efficiency, but rather to preserve the state-estimation independence of each region in a multi-regional electric energy system.

The proposed decentralized estimator relies on an elaborated instance of the Lagrangian relaxation technique that requires no central coordinator but just interchanges of information among neighboring regions. The particular structure of this estimation problem is exploited to derive a highly accurate and computationally efficient algorithm.

More often than not, identifying erroneous measurements is more important than increasing the accuracy level of a given estimation algorithm. This is so because "good" and "bad" estimators produce good enough estimates, provided that an error-free set of measurements is available. On the contrary, undetected erroneous measurements may significantly distort the estimate provided by the best estimator. This paper describes a decentralized bad measurement detection procedure that proves to be efficient and robust in terms of identifying erroneous measurements within regions and in border tie-lines.

B. Literature Review and Contributions

The technical literature includes a significant number of references on Multi-Area State-Estimation (MASE) algorithms. Work [1] provides a taxonomy of these methods, which can be categorized as hierarchical or decentralized.

A hierarchical MASE was first proposed in [2], providing a technique that relies on a border-bus overlapping approach. There is a significant number of posterior studies, based on parallel computation techniques [3], [4], two-level MASE with non-overlapping areas [5], diakoptic-based MASE [6], and others [7]–[10].

Other some works [11]–[15] formulate the estimator applying optimization and decomposition techniques to the original problem, leading the so-called "decentralized MASE" approaches. References [14] and [15] apply the Lagrangian decomposition technique to the Weighted Least Squares estimator formulated as an optimization problem. Specifically, [14] decomposes the estimation problem into subproblems to be solved by each region, considering that the border buses belong to two regions simultaneously and requiring central coordination. Reference [15] improves this decentralization procedure and proposes an algorithm to estimate any multi-region system without the need of having in common any border bus, and without central coordination.

This paper is based on the Lagrangian relaxation in [16] and builds upon previous decomposition approaches ([14] and [15]), presenting the following three features:

1) The structure of the multi-region problem is fully exploited to achieve regional problems that can be solved with accuracy and efficiency, to minimize the information interchanged and without the need of a central coordinator.
2) Sensitivity information of neighboring regions is exchanged, which allows formulating a set of regional problems whose optimal solution corresponds to the centralized estimate.
3) The proposed erroneous measurement identification procedure, which is decentralized and novel, reconstructs accurately the required entries of the centralized residual covariance matrix, which ensures efficiency and robustness in terms of identifying erroneous measurements within regions and in border tie-lines.

C. Paper Organization

The rest of this paper is organized as follows. Section II details the formulation for both centralized and decentralized state-estimation algorithms, and provides a technique to identify bad measurements in a decentralized fashion. In Section III the proposed decentralized estimator and bad data identification procedure are tested using the IEEE 30-bus system, and its performance is analyzed in detail. Finally, Section IV provides some relevant conclusions. An appendix shows the equivalence of the centralized and decentralized procedures.

II. Formulation

In this section, both centralized and decentralized formulations are described and a procedure to identify bad measurements in a decentralized fashion is proposed.

A. Centralized Formulation

In general, any state estimator can be formulated as an optimization problem:

$$\underset{\boldsymbol{x}}{\text{minimize}} \quad J\ (\boldsymbol{x}) \tag{1a}$$

subject to:

$$\boldsymbol{f}(\boldsymbol{x}) \quad = \quad \mathbf{0} \tag{1b}$$

$$\boldsymbol{g}(\boldsymbol{x}) \quad \leq \quad \mathbf{0} \tag{1c}$$

where $\boldsymbol{x}$ is the vector of state variables, $J(\boldsymbol{x})$ is the scalar error function of the estimation, $\boldsymbol{f}(\boldsymbol{x})$ is an equality-constraint functional vector mainly enforcing condition at zero-injection buses (no generation and no demand), and $\boldsymbol{g}(\boldsymbol{x})$ is an inequality-constraint vector modeling physical limits of the system.

The expression of the objective function $J(\boldsymbol{x})$ depends on the estimator employed. Particularly, the widely-used Weighted Least Squares (WLS) technique considers the expression below:

$$J(\boldsymbol{x}) = [\boldsymbol{h}(\boldsymbol{x}) - \boldsymbol{z}]^T \boldsymbol{W} [\boldsymbol{h}(\boldsymbol{x}) - \boldsymbol{z}] \tag{2}$$

where $\boldsymbol{z}$ is the measurement vector, $\boldsymbol{h}(\boldsymbol{x})$ is a functional vector that relates vectors $\boldsymbol{z}$ and $\boldsymbol{x}$, and $\boldsymbol{W}$ is the weighting matrix, usually computed as the inverse of the measurement variance matrix. It is assumed that the network is fully observable, which is a well-established hypothesis in the state-estimation technical literature for transmission systems.

B. Decentralized Formulation

In order to design a multi-area state estimator, Lagrangian decomposition (see [17]) can be applied to problem (1). Hereinafter, the multi-region network is divided into regions called "areas". The state variable vector in area A_i is denoted as $\boldsymbol{x}_i$ and it is divided into two vectors: $\boldsymbol{x}_i = [(\boldsymbol{x}_i^{\mathrm{I}})^T (\boldsymbol{x}_i^{\mathrm{B}})^T]^T$. Vectors $\boldsymbol{x}_i^{\mathrm{I}}$ and $\boldsymbol{x}_i^{\mathrm{B}}$ represent the state variables for interior and border buses of area A_i, respectively. The specific information contained in vector $\boldsymbol{x}_i^{\mathrm{B}}$ is detailed in Section II-C.

The objective function $J(\boldsymbol{x})$ can be decomposed per area and the state estimator for area A_i can be formulated as:

$$\underset{\boldsymbol{x}_i}{\text{minimize}} \quad J_i(\boldsymbol{x}_i) + \textstyle\sum_{j\in\Omega_{A_i}} J_{ij}(\boldsymbol{x}_i^{\mathrm{B}}, \tilde{\boldsymbol{x}}_j^{\mathrm{B}}) \tag{3a}$$

$$+ \sum_{j\in\Omega_{A_i}} \left[\boldsymbol{\lambda}_{ji}^{\mathrm{B}}\right]^T \boldsymbol{f}_{ji}(\boldsymbol{x}_i^{\mathrm{B}}, \tilde{\boldsymbol{x}}_j^{\mathrm{B}}) + \sum_{j\in\Omega_{A_i}} \left[\boldsymbol{\mu}_{ji}^{\mathrm{B}}\right]^T \boldsymbol{g}_{ji}(\boldsymbol{x}_i^{\mathrm{B}}, \tilde{\boldsymbol{x}}_j^{\mathrm{B}})$$

subject to:

$$\boldsymbol{f}_i(\boldsymbol{x}_i) = \boldsymbol{0} \tag{3b}$$

$$\boldsymbol{g}_i(\boldsymbol{x}_i) \leq \boldsymbol{0} \tag{3c}$$

$$\boldsymbol{f}_{ij}(\boldsymbol{x}_i^{\mathrm{B}}, \tilde{\boldsymbol{x}}_j^{\mathrm{B}}) = \boldsymbol{0} \quad : \quad \boldsymbol{\lambda}_{ij}^{\mathrm{B}} \tag{3d}$$

$$\boldsymbol{g}_{ij}(\boldsymbol{x}_i^{\mathrm{B}}, \tilde{\boldsymbol{x}}_j^{\mathrm{B}}) \leq \boldsymbol{0} \quad : \quad \boldsymbol{\mu}_{ij}^{\mathrm{B}} \tag{3e}$$

where $\boldsymbol{x}_i$ is the state variable vector for buses in area A_i; $\boldsymbol{x}_i^{\mathrm{B}}$ is the state variable vector for the border buses of area A_i; J_i and J_{ij} are the objective function components for measurements in the area A_i and belonging to border lines A_i-A_j, respectively; $\boldsymbol{f}_i(\cdot)$ and $\boldsymbol{g}_i(\cdot)$ are the equality and inequality constraint vectors for area A_i, respectively; $\boldsymbol{f}_{ij}(\cdot)$ and $\boldsymbol{g}_{ij}(\cdot)$ are the equality and inequality constraint vectors, respectively, for the border lines A_i-A_j; $\boldsymbol{\lambda}_{ij}^{\mathrm{B}}$ and $\boldsymbol{\mu}_{ij}^{\mathrm{B}}$ are the dual variable vectors related to the equality and inequality constraints affecting border lines, respectively. Note that the tilde denotes a constant vector.

The exchanged information is minimal: basically the estimated states for border buses and the dual variable values for border equality/inequality constraint (more details about the interchanged information are provided in Section II-C).

The proposed formulation extends that in [15] as it allows considering zero-injection border buses. In case of neither equality nor inequality constraints affect border variables, the objective function (3a) does not contain any dual (Lagrangian multiplier) information and, thus, the proposed formulation is simplified to the one proposed in [15].

The proposed decomposition can be applied to any estimator formulated as an optimization problem. Specifically, the proposed method is suitable for the case in which each region implements a different state-estimation procedure, provided that appropriate border information is interchanged. For conciseness, the WLS technique is considered throughout this paper. Additionally, this technique can also be applied in case of considering measurement dependencies, as in [18], [19].

Finally, it is important to note that the solution of regional problems (3) corresponds to that obtained by solving (1), as shown in the Appendix. Observe also that decentralization (3) is not oriented to reduce the computational time, but to minimize the exchanged data, preserving the independency between areas A_i. However, it is relevant to note that the Lagrangian decomposition technique used in this paper is shown to be more efficient than a centralized approach within an optimal power flow framework (see [16]).

C. Information Interchange and Convergence Improvement

To estimate the state of a multi-area system in a decentralized fashion several iterations are required. For each iteration, each area A_i solves problem (3) and interchange with the neighboring areas A_j data on: (i) border-bus estimates $\tilde{\boldsymbol{x}}_j^{\mathrm{B}}$, (ii) dual data related to border constraints $\{\tilde{\boldsymbol{\lambda}}_{ij}^{\mathrm{B}}, \tilde{\boldsymbol{\mu}}_{ij}^{\mathrm{B}}\}$, and (iii) the neighboring power measurements affecting the border lines (see Section II-E). Note that no central coordinator is required, just information interchange.

The information included in vector $\tilde{\boldsymbol{x}}_j^{\mathrm{B}}$ comprises the estimated voltage magnitudes and angles for the first-order vicinity buses. In case of zero-injection border buses, the estimates for the second-order vicinity buses are also needed. Fig. 1 provides a simple inter-area example which illustrates the exchanged information regarding state variables.

Note that border estimates and neighboring sensitivity data are required to be exchanged for the following purposes: (i) to achieve a robust and efficient convergence, and (ii) to ensure that the decentralized solution correspond to that obtained if the problem is solved in a centralized manner. Observe also that all boundary telemetry is required to be exchanged, except for the voltage magnitude/angle measurements at border buses. However, if these measurements are also transmitted to neighboring areas (as NERC standards indicate), a more accurate and robust estimate is expected, because additional information is available.

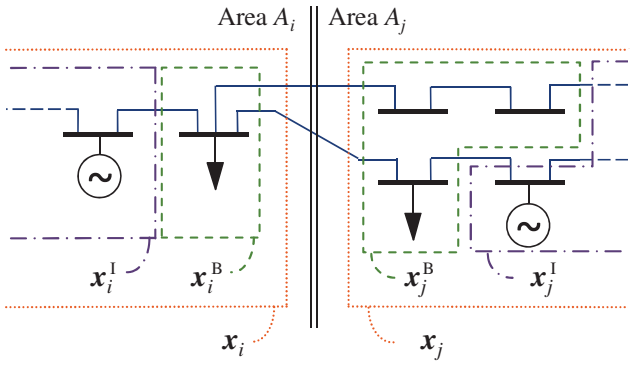

Fig. 1. Inter-area illustrative example: information interchange.

The interchanged information about neighboring estimates can be incorporated in the optimization problem (3) in several ways. In reference [20], those values are treated as fixed parameters in each estimation. Work [15] considers those estimates as measurements, and inserts them in the decentralized objective function as measurements with fixed weighting factors. In this paper, those values are treated as fixed parameters or as measurements, depending on the decentralized algorithm used (see Section II-D).

To achieve fast convergence and to reduce the number of iterations, the optimization-variables set of the proposed decentralized algorithm is modified as follows,

- The variable set of optimization problem (3) is extended from $\{\boldsymbol{x}_i\}$ to $\{\boldsymbol{x}_i, \boldsymbol{x}_j^{\mathrm{B}}\} \forall j \in \Omega_{A_i}$, just for the first iteration.
- For the rest of iterations the optimization variable set is restored: $\{\boldsymbol{x}_i\}$.

Numerical simulations indicate that proceeding in this way the algorithm converges faster than if the optimization set is defined as $\{\boldsymbol{x}_i\}$ in the first iteration.

D. Sequential and Parallel Decentralized Algorithms

The decentralized estimation problem formulated in (3) can be implemented either in a parallel fashion or in a sequential manner, as detailed below.

- Parallel: all areas solve their respective problems simultaneously, and then interchange border information.
- Sequential: areas solve their problem one at a time, and border data are updated and made available to other areas.

Fig. 2 depicts the coordination process of a two-area system employing the two alternative decentralized algorithms. In terms of exchanged information during each iteration, note that parallel and sequential decentralized procedures are analogous to Jacobi and Gauss-Seidel iterative methods for solving linear systems of equations, respectively.

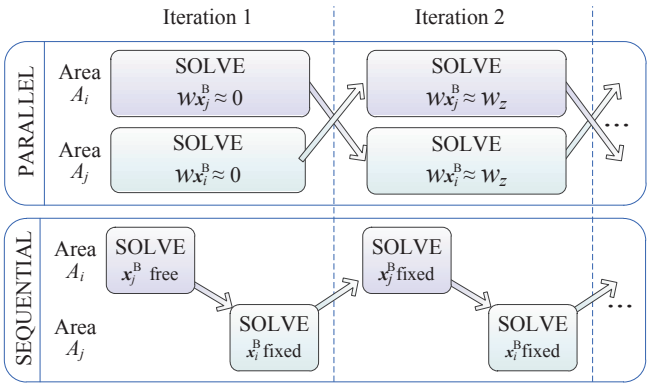

Fig. 2. Parallel and sequential decentralized algorithms.

Parallel Decentralized Algorithm. The parallel decentralized algorithm works as follows:

1) States are initialized using the flat voltage profile, and vectors $\{\tilde{\boldsymbol{\mu}}_{ji}^{\mathrm{B}}, \tilde{\boldsymbol{\lambda}}_{ji}^{\mathrm{B}}\}$ are set to zero. Set counter $\nu = 0$.
2) Set counter $\nu \leftarrow \nu + 1$. Simultaneously, each area solves problem (3). If $\nu = 1$, the optimization variable set is $\{\boldsymbol{x}_i, \boldsymbol{x}_j^{\mathrm{B}}\} \forall j \in \Omega_{A_i}$; else $\{\boldsymbol{x}_i\}$.
3) If the maximum change of the states within two iterations is smaller than a tolerance ε, stop. Else, continue.
4) Neighboring areas interchange the estimates $\tilde{\boldsymbol{x}}_i^{\mathrm{B}}$ and the dual information $\{\tilde{\boldsymbol{\mu}}_{ji}^{\mathrm{B}}, \tilde{\boldsymbol{\lambda}}_{ji}^{\mathrm{B}}\}$. Go to step 2).

Sequential Decentralized Algorithm. The sequential decentralized algorithm works as follows:

1) States are initialized using the flat voltage profile, and vectors $\{\tilde{\boldsymbol{\mu}}_{ji}^{\mathrm{B}}, \tilde{\boldsymbol{\lambda}}_{ji}^{\mathrm{B}}\}$ are set to zero. Set counter $\nu = 0$.
2) Set counters $\nu \leftarrow \nu + 1$ and $i = A_1$.
3) Area A_i solves problem (3). If $\nu = 1$ and $i = A_1$, the optimization variable set is $\{\boldsymbol{x}_i, \boldsymbol{x}_j^{\mathrm{B}}\}\ \forall j \in \Omega_{A_i}$; else, the optimization variable set is $\{\boldsymbol{x}_i\}$.
4) Area A_i interchanges the estimates $\tilde{\boldsymbol{x}}_i^{\mathrm{B}}$ and the dual information $\{\tilde{\boldsymbol{\mu}}_{ji}^{\mathrm{B}}, \tilde{\boldsymbol{\lambda}}_{ji}^{\mathrm{B}}\}\ \forall j \in \Omega_{A_i}$. If $A_i \neq A_{n_A}$, set $i \leftarrow i + 1$ and go to step 3). Otherwise, continue.
5) If the maximum change of the state variables within two iterations is smaller than a tolerance ε, stop. Otherwise, go to step 2).

Note that there is a tradeoff between accuracy and efficiency: using a smaller tolerance ε, the numerical accuracy improves whereas the required CPU time increases. Thus, the numerical accuracy for the decentralized procedure is chosen by each System Operator which adjusts the tolerance ε. In Section III, the accuracy and computational performance for these two approaches are analyzed in detail.

Numerical simulations show that the sequential procedure is more efficient than the parallel one. However, the parallel version requires a smaller level of coordination.

Observe that the sequential algorithm is the "natural" way to reach the optimum, since each area solves its problem considering the most updated estimates of neighboring bus states. Thus, each problem tries to improve the neighboring estimates progressively. In the parallel technique, each area solves its problem at the same time, estimating also the neighboring buses. The estimates for the neighboring buses do not usually match in the first iterations, and areas "compete" between them to achieve the optimum.

In case of installing a set of PMUs, the reference angle is "transmitted" with the phasor measurements and, thus, the parallel algorithm improves significantly its efficiency.

E. Gross Error Detection and Identification

Bad data detection and identification procedures are performed using the Chi-square and Largest Normalized Residual (LNR) tests, respectively. These tests are well-documented in the technical literature [21].

The normalized residual vector $\boldsymbol{r}^N$ is computed as follows:

$$\boldsymbol{r}^N = |\boldsymbol{r}| / \sqrt{\mathrm{diag}(\boldsymbol{\Omega})} \quad (4)$$

$$\boldsymbol{\Omega} = \boldsymbol{W}^{-1} - \boldsymbol{H}(\boldsymbol{H}^T \boldsymbol{W} \boldsymbol{H})^{-1} \boldsymbol{H}^T \quad (5)$$

where $\boldsymbol{r}$ is the residual vector: $\boldsymbol{r} = \boldsymbol{h}(\boldsymbol{x}^*) - \boldsymbol{z}$, and $\boldsymbol{x}^*$ is the optimal estimate.

From (4), note that the calculation of the normalized residual vector $\boldsymbol{r}^N$ is based on the Jacobian matrix $\boldsymbol{H}(\boldsymbol{x})$, which in turn is used to compute the residual variance-covariance matrix $\boldsymbol{\Omega}$. The vector $\boldsymbol{r}^N$ can only be computed in a centralized manner, because the matrix $\boldsymbol{H}(\boldsymbol{x})$ must be completely known.

Thus matrix $\boldsymbol{\Omega}$ cannot be computed in an exact manner "by blocks", i.e., if we try to compute matrix $\boldsymbol{\Omega}$ in a decentralized fashion, some entries differ significantly from those obtained if $\boldsymbol{\Omega}$ is computed with full information from all areas.

Since each area A_i can compute only its Jacobian $\boldsymbol{H}_{A_i}^{\mathrm{dec}}(\boldsymbol{x}_i)$, the area A_i can only compute an approximation

of the block of $\boldsymbol{\Omega}$ corresponding to area A_i:

$$\boldsymbol{\Omega}_{A_i}^{\text{dec}} = (\boldsymbol{W}_{A_i}^{\text{dec}})^{-1} - \boldsymbol{H}_{A_i}^{\text{dec}} \left[(\boldsymbol{H}_{A_i}^{\text{dec}})^T \boldsymbol{W}_{A_i}^{\text{dec}} \boldsymbol{H}_{A_i}^{\text{dec}} \right]^{-1} (\boldsymbol{H}_{A_i}^{\text{dec}})^T \tag{6}$$

Matrix $\boldsymbol{H}_{A_i}^{\text{dec}}(\boldsymbol{x}_i)$ can be computed in several ways. Reference [15] proposes a technique to compute this matrix considering only the measurement set that belong to area A_i. In this paper, instead of considering only the measurements contained in area A_i, we take into account all measurements whose Jacobian elements have influence over the state variables in area A_i. Thus, the measurements considered in the computation of $\boldsymbol{H}_{A_i}^{\text{dec}}(\boldsymbol{x}_i)$ are: the measurements contained in area A_i, the power flow measurements in border lines (if any), and the power injection measurements in first-order neighboring buses (if any). Additionally, instead of considering only the state variables of area A_i, the information about the neighboring estimates $\boldsymbol{x}_j^{\text{B},*}$ can also be used to expand the Jacobian. Proceeding in this way, all the available information is employed in the computation of the decentralized Jacobian and, thus, it is expected an accuracy improvement. In Section III-B, numerical analysis are carried out to check the performance of the proposed method.

Fig. 3 depicts the structure of the Jacobian $\boldsymbol{H}(\boldsymbol{x})$ for a two-areas system. The gray-colored regions represent the non-zero elements, and the dotted lines highlight the considered elements for the approach employed in [15] and the one proposed in this paper (labeled using the superscripts DEC1 and DEC2, respectively).

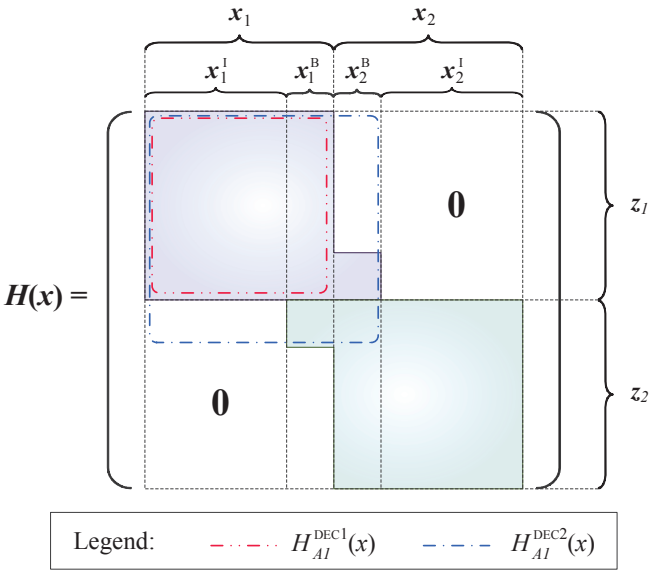

Fig. 3. Jacobian for a two-areas network.

F. Topological Errors

If the status of one or more breakers is misidentified and transmitted to the EMS, it provokes a topological error which has to be detected and corrected to achieve an accurate estimate. There are a significant number of references in the technical literature addressing the problem of topological error identification [22]–[27].

The work reported in [24] proposes a topological error identification procedure based on Lagrangian multipliers. This method is computationally efficient, robust, and can be implemented in a decentralized fashion. Thus, each area performs the decentralized estimation and, then, the topological error identification and bad data detection/identification procedures, considering only its local network.

If topological errors are located in border substations, the proposed decentralization technique allows their correct identification, since neighboring areas interchange the Lagrange multipliers corresponding to border-bus constraints.

For the sake of simplicity, the case study reported in section III-C do not consider this type of error.

III. Case Study

In this section, the proposed decentralized estimation procedure is applied to the IEEE 30-bus system [28]. This network, depicted in Fig. 4, is composed by 30 buses, 41 lines, 6 generators, 20 loads, and 6 zero-injection buses.

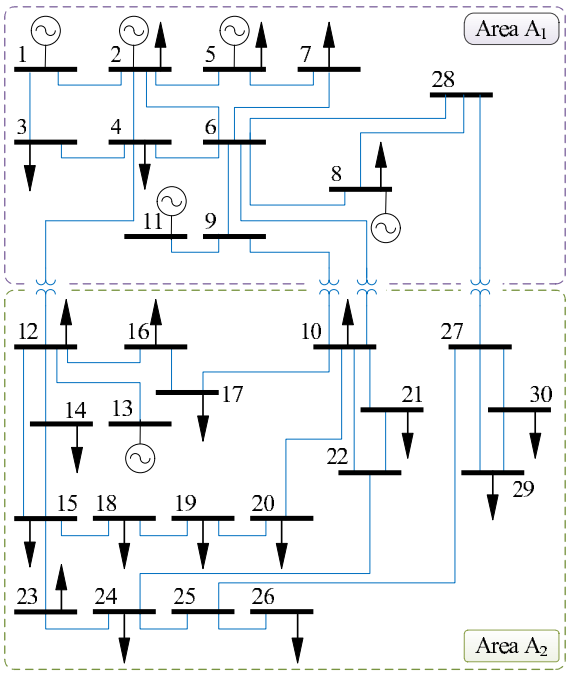

Fig. 4. IEEE 30-bus system.

The selected network is divided into two areas (see Fig. 4). Table I provides a detailed description of each area.

TABLE I
Network Description.

	Area 1	Area 2
No. of buses	11	19
No. of lines	14	23
Buses (Ω_{A_i})	{1–9, 11, 28}	{10, 12–27, 29, 30}
Zero-injection buses	{6, 9, 28}	{22, 25, 27}
Border buses	{4, 6, 9, 28}	{10, 12, 27}
Exchanged dual info.	$\{\lambda_6^{\text{B}}, \lambda_9^{\text{B}}, \lambda_{28}^{\text{B}}\}$	$\{\lambda_{27}^{\text{B}}\}$
Border lines	{ 4–12, 6–10, 9–10, 27–28 }	

For statistical consistency, each performance analysis is carried out considering one hundred measurement scenarios. Each scenario involves: (i) a random load level (from 90% to 110%); (ii) random locations of voltage measurements, active/reactive power flow measurements, and active/reactive power injection measurements (ensuring observability of the whole system); (iii) a random redundancy level (from 2.9 to 3.7); and (iv) Gaussian-distributed errors in all measurements, (standard deviation of 0.01 and 0.02 p.u. for voltage and power measurements, respectively). Each measurement scenario is synthetically generated from the solution of a converged power flow by adding Gaussian-distributed errors to the corresponding true values. The reference angle is located at bus 1.

The computational analyses reported below have been performed using MINOS 5.5 [29] under GAMS [30] on a Linux-based server with eight processors clocking at 2.3 GHz and 8 GB of RAM. Tolerance ε is set to 10^{-4}.

A. Computational Performance

In this subsection, the accuracy and convergence of the proposed decentralized estimators (sequential and parallel) are analyzed and compared with a centralized estimation algorithm. No gross errors are considered in this first study.

To compare the accuracy provided by the decentralized estimator with respect to the centralized one for the scenario ω, the metrics $\epsilon^{V}_{\text{abs},\omega}$ and $\epsilon^{\theta}_{\text{abs},\omega}$ are defined as:

$$\epsilon^{V}_{\text{abs},\omega} = \text{mean}(\boldsymbol{V}^{\text{cen}} - \boldsymbol{V}^{\text{dec}}) \tag{7}$$

$$\epsilon^{\theta}_{\text{abs},\omega} = \text{mean}(\boldsymbol{\theta}^{\text{cen}} - \boldsymbol{\theta}^{\text{dec}}) \, . \tag{8}$$

Note that $\epsilon^{V}_{\text{abs},\omega}$ ($\epsilon^{V}_{\text{abs},\omega}$) is the average absolute error of the decentralized voltage-magnitude (voltage-angle) estimates compared with the centralized ones for scenario ω.

Considering one hundred scenarios, Table II provides the following computational results: average number of iterations, average time for each iteration, average total time, and mean of $\epsilon^{V}_{\text{abs},\omega}$ and $\epsilon^{\theta}_{\text{abs},\omega}$.

TABLE II
COMPUTATIONAL ANALYSIS RESULTS.

		Centralized	Sequential	Parallel
Avg. no. of iterations		–	9	23
Avg. time for iteration	(s)	0.056	0.025	0.031
Avg. total time	(s)	0.056	0.207	0.720
$\text{mean}(\epsilon^{\text{V}}_{\text{abs},\omega})$	(p.u.)	-	0.0002	0.0011
$\text{mean}(\epsilon^{\theta}_{\text{abs},\omega})$	(rad)	-	0.0004	0.0021

From Table II, the following observations are in order:

1) The accuracy of the decentralized algorithms is adequate and the number of required iterations is around 10 for the sequential procedure, and 20 for the parallel one.
2) As expected, each decentralized subproblem is faster to solve than the centralized one. The decentralized average time per iteration is smaller than the corresponding to the time required to solve the centralized problem. On the other hand, the total estimation time is about ten times higher for the decentralized procedures.
3) The accuracy provided by both procedures is high, being the sequential estimates closer to the centralized ones.

Based on the previous study, two additional cases are analyzed. In "Case 2A", two PMUs are included in the metering infrastructure, and located at buses 2 and 25 (see Fig. 4). It is assumed that these GPS-synchronized devices provide voltage-magnitude and voltage-angle measurements subjected to an error with a standard deviation of 0.005 pu. In "Case 2B", no PMUs are included and the standard deviations of traditional measurements are increased up to 0.05 and 0.02 p.u. for power and voltage measurements, respectively. The computational results for both cases are reported in Table III.

TABLE III
COMPUTATIONAL ANALYSIS RESULTS (SEE UNITS IN TABLE II).

	Case 2A			Case 2B		
	Centr.	Seq.	Par.	Centr.	Seq.	Par.
No. of iter.	–	9	9	–	13	32
Avg. time	0.047	0.019	0.027	0.047	0.019	0.025
Total time	0.047	0.174	0.248	0.047	0.245	0.804
$\text{mean}(\epsilon^{\text{V}}_{\text{abs}})$	–	0.0002	0.0009	–	0.0002	0.0021
$\text{mean}(\epsilon^{\theta}_{\text{abs}})$	–	0.0002	0.0015	–	0.0004	0.0050

From Table III, the following observations are in order:

1) The installation of PMUs (Case 2A) improves significantly the efficiency of the parallel algorithm. Note that (i) the estimation time for the decentralized procedures is about five times higher than that for the centralized approach, and (ii) the average number of iterations for both decentralized techniques coincide.
2) On the other hand, if the error of the metering devices increases (Case 2B), both the numerical accuracy and the computational efficiency worsen. Note that the average iteration number increases for both decentralized algorithms.

Finally, the performance of the proposed method in a large system is analyzed. The IEEE 118-bus network [28] is divided into two regions (areas A_1 and A_2, which comprise 65 and 58 buses, respectively), which result in ten border tie-lines. Results using the parallel and sequential decentralized algorithms are provided in Table IV (tolerance $\varepsilon = 10^{-3}$).

TABLE IV
COMPUTATIONAL ANALYSIS RESULTS FOR THE 118-BUS CASE.

		Centralized	Sequential	Parallel
Avg. no. of iterations		–	2.6	4.6
Avg. time for iteration	(s)	0.314	0.203	0.116
Avg. total time	(s)	0.314	0.518	0.527
$\text{mean}(\epsilon^{\text{V}}_{\text{abs},\omega})$	(p.u.)	-	0.0007	0.0004
$\text{mean}(\epsilon^{\theta}_{\text{abs},\omega})$	(rad)	-	0.0024	0.0008

From Table IV the following observations are in order:

1) Although the number of iterations for the parallel algorithm is twice than that of the sequential one, the total estimation time for both algorithms is similar.
2) Note that in this case the required CPU time for the decentralized procedure is just 0.6 times higher than that of the centralized one.

3) The numerical accuracy provided by the decentralized methods is appropriate.

B. Residual Variance Calculation

As stated in Section II-E, the decentralized computation of the residual variance-covariance matrix ($\mathbf{\Omega}^{\text{cen}}$), used to normalize residuals for bad data identification, is not straightforward: it leads to an approximate matrix denoted as $\mathbf{\Omega}^{\text{dec}}$. In this subsection, the quality of this approximation is numerically analyzed and discussed. Note that only the diagonal elements of matrix $\mathbf{\Omega}$ are of interest since only these elements are required to compute normalized residuals.

To perform a comparison between the diagonal elements of $\mathbf{\Omega}^{\text{cen}}$ and $\mathbf{\Omega}^{\text{dec}}$, the IEEE 30-bus system and one hundred measurement sets are considered. The true state vector $\boldsymbol{x}^{\text{true}}$ (obtained from a converged power flow) is employed to compute both matrices $\mathbf{\Omega}^{\text{cen}}$ and $\mathbf{\Omega}^{\text{dec}}$, using (5) and (6), respectively. Once both matrices are computed for each scenario, the diagonal elements are numerically compared, analyzing separately the elements corresponding to border-line measurements and the rest. To perform the comparison, the following metrics are defined:

$$\epsilon^{\text{in}}_{\text{rel},\omega}(\%) = \text{mean}\left(100\left|\mathbf{\Omega}^{\text{cen}}_{kk} - \mathbf{\Omega}^{\text{dec}}_{kk}\right|/\mathbf{\Omega}^{\text{cen}}_{kk}\right), \forall i \in \Theta_{\text{in}} \quad (9)$$

$$\epsilon^{\text{bor}}_{\text{rel},\omega}(\%) = \text{mean}\left(100\left|\mathbf{\Omega}^{\text{cen}}_{kk} - \mathbf{\Omega}^{\text{dec}}_{kk}\right|/\mathbf{\Omega}^{\text{cen}}_{kk}\right), \forall i \in \Theta_{\text{bor}} \quad (10)$$

where Θ_{bor} is the set of measurements related to border lines and Θ_{in} is the set corresponding to the rest of measurements. Note that $\epsilon^{\text{in}}_{\text{rel},\omega}$ and $\epsilon^{\text{bor}}_{\text{rel},\omega}$ are the average relative errors of $\text{diag}(\mathbf{\Omega}^{\text{dec}})$ with respect to $\text{diag}(\mathbf{\Omega}^{\text{cen}})$ for the measurement sets Θ_{in} and Θ_{bor}, respectively, and scenario ω.

Table V provides the following statistical results: minimum, average, and maximum for both parameters $\epsilon^{\text{in}}_{\text{rel},\omega}$ and $\epsilon^{\text{bor}}_{\text{rel},\omega}$, for all measurement scenarios.

TABLE V
ACCURACY ANALYSIS RESULTS.

		$\epsilon^{\text{in}}_{\text{rel},\omega}$	$\epsilon^{\text{bor}}_{\text{rel},\omega}$
Minimum	(%)	0.78	3.61
Average	(%)	0.88	5.86
Maximum	(%)	1.00	8.34

From Table V, note that the average relative error for measurements inside the area are not significant (always below 1%). On the other hand, the average relative error for measurements corresponding to border lines is sufficiently accurate (around 6%). Exhaustive numerical simulations show that those errors increase around 150% in case of computing the Jacobian disregarding neighboring measurements affecting border lines and variables $\boldsymbol{x}^{\text{B}}_j$ (as in [15]).

In the following section, it is numerically shown that these errors are small enough to identify correctly any bad data populating the measurement set.

C. Bad Data Detection and Identification

In this section, the bad data detection and identification capabilities of the decentralized algorithms are numerically analyzed and compared with the centralized procedure.

This analysis is carried out considering that each measurement scenario is corrupted by four bad measurements randomly located, with an error-magnitude of fifteen standard deviations. Four types of location are considered:

- Error affecting a voltage measurement in border buses (labeled as "V [border]").
- Error affecting a voltage measurement in non-border buses (labeled as "V [in]").
- Error affecting an active/reactive power measurement in border lines (labeled as "P/Q [border]").
- Error affecting an active/reactive power measurement in non-border lines (labeled as "P/Q [in]").

One hundred measurement scenarios are generated and four bad measurements are randomly allocated per scenario. Results are presented in Fig. 5. The white-colored bars in Fig. 5 provide the quantity of the actual randomly-located errors (labeled as "Actual") for each type of measurement. For example, 74 bad measurements are located in voltage measurements in non-border buses.

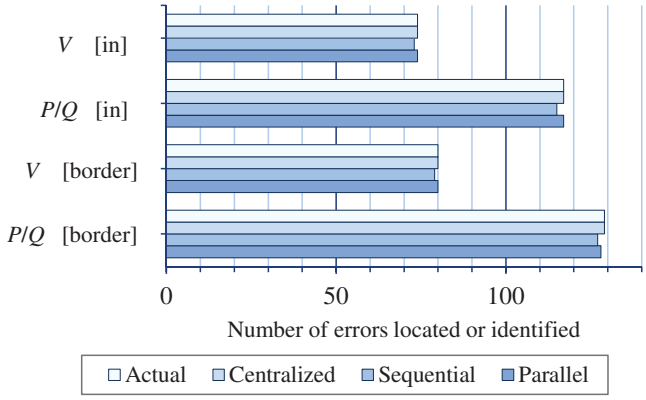

Fig. 5. Bad data identification results.

For each scenario, the detection and identification tests are applied for the centralized, decentralized-sequential, and decentralized-parallel estimators. Shadowed bars in Fig. 5 represent the total number of bad measurements correctly identified, sorted by type. For example, 74 "V [in]" errors (out of 74) are identified by the centralized algorithm, and the sequential and parallel methods identify 73 and 74 (out of 74), respectively. Note that the identification failures are due to the approximation of the residual variance-covariance matrix.

Additionally, it has been observed that the three identification methods sometimes identify as bad data some good measurements. The percentages of these misidentifications are: 3.75 %, 5.25 %, and 6.75%, for the centralized, sequential, and parallel algorithms, respectively.

Note that the performance of the proposed bad data detection and identification procedures applied to the decentralized algorithms are sufficiently accurate to identify bad measurements. Note also that the number of misidentifications for the proposed technique is similar to that of a centralized approach.

Note that the decentralized formulation allows a decentralized estimation as well as a decentralized bad data detection and identification (i.e., each area detects and identifies its own measurement/topological errors). The decentralized solution

involves solving problems comparatively smaller than the original one, which might be computationally advantageous. Moreover, this identification procedure can be performed in a parallel fashion, decreasing significantly the corresponding computational burden. For instance, if there are two gross errors in each region, the centralized algorithm has to perform four re-estimations, whereas the decentralized one only requires just two. In this respect, the CPU time reduction can be significant for systems with a larger number of areas.

IV. Conclusions

The specific instance of the Lagrangian decomposition algorithm used in this paper to carry out a decentralized state estimation is accurate, as it achieves in a few iterations the same estimation than that obtained by a centralized algorithm. This is so for both the sequential and the parallel implementations. Since the sequential implantation considers all the available information regarding previously solved problems, it is computationally more efficient than the parallel implementation. However, the sequential implementation requires coordination among areas.

The proposed technique to compute in a decentralized manner the relevant entries of the residual variance-covariance matrix is sufficiently accurate to achieve the identification of bad measurements involving both intra-area and border measurements. Moreover, it is reliable as the number of misidentifications for the proposed technique is similar to that of a centralized approach.

The accuracy of the proposed estimator and its ability to identify bad measurements (within each area and in border lines) is proved by a large number of simulations, which allows drawing statistically sounds conclusions.

Appendix

A. Centralized KKT

The objective function in problem (1) can be expanded:

$$J(\boldsymbol{x}) \;=\; \sum_{i=1}^{n_A} J_i(\boldsymbol{x}_i) + \sum_{i=1}^{n_A} \sum_{j\in\Omega_{A_i}} J_{ij}(\boldsymbol{x}_i^{\mathrm{B}}, \boldsymbol{x}_j^{\mathrm{B}})\,. \tag{11a}$$

Similarly, constrains (1b)–(1c) can be expressed as:

$$\left.\begin{array}{rcl} \boldsymbol{f}_i(\boldsymbol{x}_i) &=& \mathbf{0} \;:\; \boldsymbol{\lambda}_i \\ \boldsymbol{g}_i(\boldsymbol{x}_i) &\le& \mathbf{0} \;:\; \boldsymbol{\mu}_i \end{array}\right\} \forall i \tag{11b}$$

$$\left.\begin{array}{rcl} \boldsymbol{f}_{ij}(\boldsymbol{x}_i^{\mathrm{B}}, \boldsymbol{x}_j^{\mathrm{B}}) &=& \mathbf{0} \;:\; \boldsymbol{\lambda}_{ij}^{\mathrm{B}} \\ \boldsymbol{g}_{ij}(\boldsymbol{x}_i^{\mathrm{B}}, \boldsymbol{x}_j^{\mathrm{B}}) &\le& \mathbf{0} \;:\; \boldsymbol{\mu}_{ij}^{\mathrm{B}} \end{array}\right\} \forall i, \forall j \in \Omega_{A_i}\,. \tag{11c}$$

Note that problem (11) is equivalent to (1). Constraints (11c) are the complicating constraints, i.e., constraints that, if relaxed, make problem (11) solvable in a decentralized manner. Optimization variables are $\boldsymbol{x} = \{\boldsymbol{x}_1, \cdots, \boldsymbol{x}_{n_A}\}$.

The KKT optimality conditions of problem (11) at the optimum $\{\boldsymbol{x}_i^*, \boldsymbol{x}_j^*, \boldsymbol{\lambda}_i^*, \boldsymbol{\mu}_i^*, \boldsymbol{\lambda}_{ij}^{\mathrm{B},*}, \boldsymbol{\mu}_{ij}^{\mathrm{B},*}\}$ are:

$$\left.\begin{array}{rcl} \mathbf{0} &=& \nabla_{x_i} J_i(\boldsymbol{x}_i^*) + \sum\limits_{j\in\Omega_i} \nabla_{x_i} J_{ij}(\boldsymbol{x}_i^{\mathrm{B},*}, \boldsymbol{x}_j^{\mathrm{B},*}) \\ &+& [\boldsymbol{\lambda}_i^*]^T \nabla_{x_i} \boldsymbol{f}_i(\boldsymbol{x}_i^*) + [\boldsymbol{\mu}_i^*]^T \nabla_{x_i} \boldsymbol{g}_i(\boldsymbol{x}_i^*) \\ &+& \sum\limits_{j\in\Omega_{A_i}} \Big[[\boldsymbol{\lambda}_{ij}^{\mathrm{B},*}]^T \nabla_{x_i} \boldsymbol{f}_{ij}(\boldsymbol{x}_i^{\mathrm{B},*}, \boldsymbol{x}_j^{\mathrm{B},*}) \\ &&\quad + [\boldsymbol{\lambda}_{ji}^{\mathrm{B},*}]^T \nabla_{x_i} \boldsymbol{f}_{ji}(\boldsymbol{x}_i^{\mathrm{B},*}, \boldsymbol{x}_j^{\mathrm{B},*}) \Big] \\ &+& \sum\limits_{j\in\Omega_{A_i}} \Big[[\boldsymbol{\mu}_{ij}^{\mathrm{B},*}]^T \nabla_{x_i} \boldsymbol{g}_{ij}(\boldsymbol{x}_i^{\mathrm{B},*}, \boldsymbol{x}_j^{\mathrm{B},*}) \\ &&\quad + [\boldsymbol{\mu}_{ji}^{\mathrm{B},*}]^T \nabla_{x_i} \boldsymbol{g}_{ji}(\boldsymbol{x}_i^{\mathrm{B},*}, \boldsymbol{x}_j^{\mathrm{B},*}) \Big] \end{array}\right\} \forall i \tag{12}$$

$$\left.\begin{array}{rcl} \boldsymbol{f}_i(\boldsymbol{x}_i^*) &=& \mathbf{0} \\ \boldsymbol{g}_i(\boldsymbol{x}_i^*) &\le& \mathbf{0} \\ [\boldsymbol{\mu}_i^*]^T \boldsymbol{g}_i(\boldsymbol{x}_i^*) &=& \mathbf{0} \\ \boldsymbol{\mu}_i^* &\ge& \mathbf{0} \end{array}\right\} \forall i \tag{13}$$

$$\left.\begin{array}{rcl} \boldsymbol{f}_{ij}(\boldsymbol{x}_i^{\mathrm{B},*}, \boldsymbol{x}_j^{\mathrm{B},*}) &=& \mathbf{0} \\ \boldsymbol{g}_{ij}(\boldsymbol{x}_i^{\mathrm{B},*}, \boldsymbol{x}_j^{\mathrm{B},*}) &\le& \mathbf{0} \\ [\boldsymbol{\mu}_{ij}^{\mathrm{B},*}]^T \boldsymbol{g}_{ij}(\boldsymbol{x}_i^{\mathrm{B},*}, \boldsymbol{x}_j^{\mathrm{B},*}) &=& \mathbf{0} \\ \boldsymbol{\mu}_{ij}^{\mathrm{B},*} &\ge& \mathbf{0} \end{array}\right\} \forall i, \forall j \in \Omega_{A_i} \tag{14}$$

B. Decentralized KKT

The problem of area A_i at the optimum for all other areas:

$$\underset{\boldsymbol{x}_i}{\text{minimize}} \quad J_i(\boldsymbol{x}_i) + \sum_{j\in\Omega_{A_i}} J_{ij}(\boldsymbol{x}_i^{\mathrm{B}}, \boldsymbol{x}_j^{\mathrm{B},*}) \tag{15a}$$
$$+ \sum_{j\in\Omega_{A_i}} [\boldsymbol{\lambda}_{ji}^{\mathrm{B},*}]^T \boldsymbol{f}_{ji}(\boldsymbol{x}_i^{\mathrm{B},*}, \boldsymbol{x}_j^{\mathrm{B}}) + \sum_{j\in\Omega_{A_i}} [\boldsymbol{\mu}_{ji}^{\mathrm{B},*}]^T \boldsymbol{g}_{ji}(\boldsymbol{x}_i^{\mathrm{B},*}, \boldsymbol{x}_j^{\mathrm{B}})$$

subject to:

$$\boldsymbol{f}_i(\boldsymbol{x}_i) \;=\; \mathbf{0} \;:\; \boldsymbol{\lambda}_i \tag{15b}$$
$$\boldsymbol{g}_i(\boldsymbol{x}_i) \;\le\; \mathbf{0} \;:\; \boldsymbol{\mu}_i \tag{15c}$$
$$\boldsymbol{f}_{ij}(\boldsymbol{x}_i^{\mathrm{B}}, \boldsymbol{x}_j^{\mathrm{B},*}) \;=\; \mathbf{0} \;:\; \boldsymbol{\lambda}_{ij}^{\mathrm{B}}, \forall j \in \Omega_{A_i} \tag{15d}$$
$$\boldsymbol{g}_{ij}(\boldsymbol{x}_i^{\mathrm{B}}, \boldsymbol{x}_j^{\mathrm{B},*}) \;\le\; \mathbf{0} \;:\; \boldsymbol{\mu}_{ij}^{\mathrm{B}}, \forall j \in \Omega_{A_i} \tag{15e}$$

The KKT optimality conditions of problem (15) for area A_i at the optimum state $\boldsymbol{x}_i^*$ are:

$$\begin{array}{rcl} \mathbf{0} &=& \nabla_{x_i} J_i(\boldsymbol{x}_i^*) + \sum\limits_{j\in\Omega_{A_i}} \nabla_{x_i} J_{ij}(\boldsymbol{x}_i^{\mathrm{B},*}, \boldsymbol{x}_j^{\mathrm{B},*}) \\ &+& [\boldsymbol{\lambda}_i^*]^T \nabla_{x_i} \boldsymbol{f}_i(\boldsymbol{x}_i^*) + [\boldsymbol{\mu}_i^*]^T \nabla_{x_i} \boldsymbol{g}_i(\boldsymbol{x}_i^*) \\ &+& \sum\limits_{j\in\Omega_{A_i}} [\boldsymbol{\lambda}_{ij}^*]^T \nabla_{x_i} \boldsymbol{f}_{ij}(\boldsymbol{x}_i^*, \boldsymbol{x}_j^*) \\ &+& \sum\limits_{j\in\Omega_{A_i}} [\boldsymbol{\lambda}_{ji}^{\mathrm{B},*}]^T \nabla_{x_i} \boldsymbol{f}_{ji}(\boldsymbol{x}_i^{\mathrm{B},*}, \boldsymbol{x}_j^{\mathrm{B},*}) \\ &+& \sum\limits_{j\in\Omega_{A_i}} [\boldsymbol{\mu}_{ij}^{\mathrm{B},*}]^T \nabla_{x_i} \boldsymbol{g}_{ij}(\boldsymbol{x}_i^{\mathrm{B},*}, \boldsymbol{x}_j^{\mathrm{B},*}) \\ &+& \sum\limits_{j\in\Omega_{A_i}} [\boldsymbol{\mu}_{ji}^{\mathrm{B},*}]^T \nabla_{x_i} \boldsymbol{g}_{ji}(\boldsymbol{x}_i^{\mathrm{B},*}, \boldsymbol{x}_j^{\mathrm{B},*}) \end{array} \tag{16}$$

$$\boldsymbol{f}_i(\boldsymbol{x}_i^*) = \mathbf{0} \quad (17)$$
$$\boldsymbol{g}_i(\boldsymbol{x}_i^*) \leq \mathbf{0} \quad (18)$$
$$(\boldsymbol{\mu}_i^*)^T \boldsymbol{g}_i(\boldsymbol{x}_i^*) = \mathbf{0} \quad (19)$$
$$\boldsymbol{\mu}_i^* \geq \mathbf{0} \quad (20)$$
$$\boldsymbol{f}_{ij}(\boldsymbol{x}_i^{\mathrm{B},*}, \boldsymbol{x}_j^{\mathrm{B},*}) = \mathbf{0}, \forall j \in \Omega_{A_i} \quad (21)$$
$$\boldsymbol{g}_{ij}(\boldsymbol{x}_i^{\mathrm{B},*}, \boldsymbol{x}_j^{\mathrm{B},*}) \leq \mathbf{0}, \forall j \in \Omega_{A_i} \quad (22)$$
$$(\boldsymbol{\mu}_{ij}^{\mathrm{B},*})^T \boldsymbol{g}_{ij}(\boldsymbol{x}_i^{\mathrm{B},*}, \boldsymbol{x}_j^{\mathrm{B},*}) = \mathbf{0}, \forall j \in \Omega_{A_i} \quad (23)$$
$$\boldsymbol{\mu}_{ij}^{\mathrm{B},*} \geq \mathbf{0}, \forall j \in \Omega_{A_i} \quad (24)$$

Considering jointly the optimality conditions (16)–(24) for all areas renders conditions (12)–(14), which proves that the centralized and decentralized formulations are equivalent.

REFERENCES

[1] A. Gómez-Expósito, A. de la Villa Jaén, C. Gómez-Quiles, P. Rousseaux, and T. V. Cutsem, "A taxonomy of multi-area state estimation methods," *Elec. Power Syst. Res.*, vol. In Press, Corrected Proof, 2010.

[2] K. Clements, O. Denison, and R. Ringlee, "A multi-area approach to state estimation in power system networks," in *IEEE PES Summer Meeting*, 1972.

[3] Y. Wallach, E. Handschin, and C. Bongers, "An efficient parallel processing method for power system state estimation," *IEEE Trans. Power App. Syst.*, no. 11, pp. 4402–4406, 1981.

[4] C. W. Brice and R. K. Cavin, "Multiprocessor static state estimation," *IEEE Trans. Power App. Syst.*, no. 2, pp. 302–308, 1982.

[5] T. Van Cutsem, J. L. Horward, and M. Ribbens-Pavella, "A two-level static state estimator for electric power systems," *IEEE Trans. Power App. Syst.*, vol. PAS-100, no. 8, pp. 3722–3732, Aug. 1981.

[6] W. Jiang, V. Vittal, and G. T. Heydt, "Diakoptic state estimation using phasor measurement units," *IEEE Trans. Power Syst.*, vol. 23, no. 4, pp. 1580–1589, Nov. 2008.

[7] S. Iwamoto, M. Kusano, and V. H. Quintana, "Hierarchical state estimation using a fast rectangular-coordinate method," *IEEE Trans. Power Syst.*, vol. 4, no. 3, pp. 870–879, Aug. 1989.

[8] L. Zhao and A. Abur, "Multiarea state estimation using synchronized phasor measurements," *IEEE Trans. Power Syst.*, vol. 20, no. 2, pp. 611–617, May 2005.

[9] W. Jiang, V. Vittal, and G. T. Heydt, "A distributed state estimator utilizing synchronized phasor measurements," *IEEE Trans. Power Syst.*, vol. 22, no. 2, pp. 563–571, May 2007.

[10] A. Gómez-Expósito and A. de la Villa Jaén, "Two-level state estimation with local measurement pre-processing," *IEEE Trans. Power Syst.*, vol. 24, no. 2, pp. 676–684, 2009.

[11] A. El-Keib, J. Nieplocha, H. Singh, and D. J. Maratukulam, "A decomposed state estimation technique suitable for parallel processor implementation," *IEEE Trans. Power Syst.*, vol. 7, no. 3, pp. 1088–1097, Aug. 1992.

[12] S. Y. Lin, "A distributed state estimator for electric power systems," *IEEE Trans. Power Syst.*, vol. 7, no. 2, pp. 551–557, May 1992.

[13] D. M. Falcao, F. Wu, and L. Murphy, "Parallel and distributed state estimation," *IEEE Trans. Power Syst.*, vol. 10, no. 2, pp. 724–730, May 1995.

[14] R. Ebrahimian and R. Baldick, "State estimation distributed processing," *IEEE Trans. Power Syst.*, vol. 15, no. 4, pp. 1240–1246, Nov. 2000.

[15] A. J. Conejo, S. de la Torre, and M. Cañas, "An optimization approach to multiarea state estimation," *IEEE Trans. Power Syst.*, vol. 22, no. 1, pp. 213–221, Feb. 2007.

[16] A. J. Conejo, F. J. Nogales, and F. J. Prieto, "A decomposition procedure based on approximate Newton directions," *Math. Program.*, vol. 93, no. 3, pp. 495–515, Dec. 2002.

[17] A. J. Conejo, E. Castillo, R. Mínguez, and R. García-Bertrand, *Decomposition techniques in mathematical programming. Engineering and science applications*. Springer, 2006.

[18] E. Caro, A. J. Conejo, and R. Mínguez, "Power system state estimation considering measurement dependencies," *IEEE Trans. Power Syst.*, vol. 24, no. 4, pp. 1875–1885, Nov. 2009.

[19] E. Caro, A. J. Conejo, R. Mínguez, M. Zima, and G. Andersson "Multiple bad data identification considering measurement dependencies," *IEEE Trans. Power Sys.*, Accepted for publication, 2011.

[20] E. Caro, A. J. Conejo, and R. Mínguez, *Optimization Advances in Electric Power Systems*. Nova Science Publishers, Inc., 2008, ch. A Mathematical Programming Approach to State Estimation, pp. 1–26.

[21] A. Abur and A. G. Expósito, *Electric Power System State Estimation. Theory and Implementations*. Marcel Dekker, 2004.

[22] M.R. Irving and M.J. Sterling, "Substation data validation", *Proceedings of IEE*, vol. 129, part C, no. 3, pp. 119-122, May 1982.

[23] K.A. Clements and P. W. Davis, "Detection and identification of topology errors in electric power systems", *IEEE Trans. on Power Syst.*, vol. 3, no. 4, pp. 1748-1753, Nov. 1988.

[24] K.A. Clements and A. Simões-Costa, "Topology error identification using normalized lagrange multipliers", *IEEE Trans. on Power Syst.*, vol. 13, no. 2, pp. 347-353, May 1998.

[25] A. Gómez-Expósito and A. Villa, "Reduced substation models for generalized state estimation", *IEEE Trans. on Power Syst.*, vol. 16, no. 4, pp. 839-846, Nov. 2001.

[26] A. Villa and A. Gómez-Expósito, "Implicitly constrained substation model for state estimation", *IEEE Trans. on Power Syst.*, vol. 17, no. 3, pp. 850-856, Aug. 2002.

[27] E. Caro, A. J. Conejo, and A. Abur, "Breaker status identification", *IEEE Trans. on Power Syst.*, vol. 25, no. 2, pp. 694-702, May 2010.

[28] Power Systems Test Case Archive. Available on: *http://www.ee.washington.edu/research/pstca/*.

[29] B. A. Murtagh, M. A. Saunders, W. Murray, P. E. Gill, R. Raman, and E. Kalvelagen, *MINOS: A solver for large-scale nonlinear optimization problems. The Solvers Manual.*, GAMS Development Corporation, Washington, DC, 2008.

[30] A. Brooke, D. Kendrick, and A. Meeraus, *Release 2.25 GAMS A User's Guide*, South San Francisco, 1992.

Eduardo Caro (S'08) received from the Polytechnical Univ. of Cataluña, Barcelona, Spain, the Electrical Engineering degree in 2007. He is currently a Ph.D. student at the Univ. of Castilla–La Mancha, Ciudad Real, Spain.

His research interests include power system state estimation, optimization, sensitivity analysis, and power system quality.

Antonio J. Conejo (F'04) received the M.S. degree from MIT, Cambridge, MA, in 1987, and a Ph.D. degree from the Royal Institute of Technology, Stockholm, Sweden in 1990. He is currently a full Professor at the Universidad de Castilla–La Mancha, Ciudad Real, Spain.

His research interests include control, operations, planning and economics of electric energy systems, as well as statistics and optimization theory and its applications.

Roberto Mínguez received from the University of Cantabria, Santander, Spain, the Civil Engineering degree, and the Ph.D. degree in Applied Mathematics and Computer Science in September 2000 and June 2003, respectively. During 2004 he worked as Visiting Scholar at Cornell University, New York, under the Fulbright program. He is currently an Assistant Professor at the Environmental Hydraulics Institute, IH, Univ. de Cantabria, Cantabria, Spain.

His research interests are reliability engineering, sensitivity analysis, and numerical methods.